Croatian Society for Materials Protection

Metalurgija/Metallurgy

Vol. 65 No. 4 / 2026

Study on thermal deformation behavior and constitutive model of 316 stainless steel for lightning rod of ancient buildings

Tong Xu [1] and Jia Zhang [2,*]

https://doi.org/10.64486/m.65.4.11

[1] Shaoxing University, Shaoxing, Zhejiang, China; xutong_112@163.com
[2] Mobile Communications Group Zhejiang Co., Ltd. Shaoxing Branch, Shaoxing, Zhejiang, China
* Correspondence: 15068518555@139.com

Type of the Paper: Article
Received: November 13, 2025
Accepted: April 17, 2026

Abstract: To address the specific performance requirements of lightning protection materials for ancient buildings, isothermal hot compression experiments were conducted with forged 316LN austenitic stainless steel employing a Gleeble-3500 thermal-mechanical simulator. The test matrix covered a strain rate range of (0.001–1) s^{-1}, a deformation temperature interval of (1273–1423) K, and a maximum true strain of 0.7, targeting a comprehensive exploration of the material's high-temperature flow behaviors. A flow stress constitutive model was constructed by integrating the Arrhenius equation, and its predictive performance was validated through rigorous comparison with experimental data. Key observations indicate that under constant strain rate conditions, elevated deformation temperatures lead to reduced compressive stress in the material. This phenomenon is closely linked to enhanced atomic mobility and accelerated dynamic recrystallization, which collectively induce softening effects. In contrast, at a fixed temperature, higher strain rates result in increased compressive stress, as rapid deformation intensifies work hardening to an extent that outweighs dynamic softening. The true stress-true strain curves exhibit a distinct three-stage evolution, rapid ascent, gradual growth, and stabilization with the final stable phase arising from a dynamic equilibrium between work hardening and dynamic softening mechanisms. This research delivers essential theoretical foundations and practical engineering guidance for refining the hot working processes of 316LN stainless steel specifically tailored to the fabrication of ancient building lightning protection systems.

Keywords: 316LN stainless steel; ancient building lightning rods; high-temperature deformation behavior; constitutive modeling; Arrhenius equation

1. Introduction

Lightning protection systems serve as a critical defense against lightning-induced damage to ancient buildings, and their long-term operational safety and durability are predominantly governed by the metallurgical performance of the core material. 316LN austenitic stainless steel has emerged as the optimal selection for this application, owing to its exceptional corrosion resistance, consistent mechanical strength, and robust adaptability to diverse environmental conditions [1–3]. The synergistic effects of its chemical composition—most notably the balanced ratios of chromium, nickel, and molybdenum-not only ensure superior corrosion resistance and high-temperature stability but also align with the "minimum intervention" principle in cultural heritage

preservation. This alignment effectively mitigates the risk of secondary pollution that may arise from the corrosion of traditional metallic materials commonly used in such applications [4–6].

Thermomechanical processing methods, including hot forging and hot bending, are indispensable in the manufacturing of lightning protection components. The metallurgical responses of materials during thermal deformation directly govern the final quality and service reliability of the finished products. Suboptimal processing parameters can give rise to a range of metallurgical defects, such as grain coarsening, crack initiation, and stress concentration, which significantly compromise the material's mechanical properties and resistance to failure [7]. Constitutive models act as fundamental tools for describing the interrelationships between stress, strain, temperature, and strain rate during thermal deformation. Their development must be firmly grounded in the intrinsic metallurgical mechanisms of the material, as their reliability directly impacts the optimization of thermomechanical processes and the accurate prediction of component performance [8–12].

Numerous studies have been conducted worldwide to explore the thermal deformation behavior of 316LN stainless steel. Researchers have leveraged the Arrhenius equation and its modified variants, in conjunction with metallurgical thermodynamics and kinetics analyses, to determine the activation energy for hot deformation and establish constitutive equations that effectively capture the material's inherent thermal deformation mechanisms [13–15]. For example, Han et al. [16] identified an optimal parameter window (1273–1473) K, (0.001–1) s^{-1} for the thermomechanical processing of 316LN stainless steel, which helps suppress undesirable microstructural changes. Xiao et al. [17] addressed the issue of distorted metallurgical information caused by "barreling" deformation during hot compression tests. They implemented a data correction approach proposed by Ebrahimi et al. [18] to eliminate frictional interference in flow stress measurements, thereby enabling a more accurate characterization of the material's true deformation behavior.

Building upon these prior advancements, the present study employs a Gleeble-3500 thermal simulation testing machine to investigate the high-temperature flow behavior of 316LN austenitic stainless steel within the aforementioned optimal parameter range. By integrating the metallurgical evolution characteristics of cylindrical specimens during thermal deformation, 16 sets of experimental data were systematically analyzed to develop a mechanism-based flow stress constitutive model. The reliability of the proposed model was verified through experimental validation, and additional confirmation was obtained via numerical simulation analysis. This work provides valuable theoretical support for the metallurgical quality control of 316LN stainless steel during the thermomechanical processing of lightning protection components specifically designed for ancient buildings.

2. Materials and Experimental Procedures

2.1 Test Material

The test material selected for this study was 316LN stainless steel, and its key chemical composition (including C, Si, P, Mo, and Ni) is presented in Table 1. This material is known for its excellent processability and can be further strengthened through heat treatment. The raw 316LN stainless steel was precision-machined into cylindrical specimens with a diameter of 8 mm and a height of 12 mm, and subsequent hot compression tests were conducted using a Gleeble-3500 thermal simulation tester.

Table 1. Chemical Composition of 316LN Stainless Steel (Mass Fraction/%)

C	Si	Mn	P	S	Ni	Cr	Cu	Mo	N	Co
0.018	0.35	0.71	0.02	0.001	11.16	15.26	0.1	2.03	0.133	0.051

2.2 Experimental Setup and Procedures

Gleeble-3500 thermal simulation testing equipment was utilized to conduct hot compression experiments. A full-factorial test design was employed, integrating four deformation temperatures (1273 K, 1323 K, 1373 K, 1423 K) with four strain rates (0.001 s^{-1}, 0.01 s^{-1}, 0.1 s^{-1}, 1 s^{-1}), leading to 16 unique experimental configurations in total. To mitigate the unfavorable impacts of end friction between the specimen and punches, a thin and

https://doi.org/10.64486/m.65.4.11

uniform coat of graphite lubricant was applied to both end surfaces of each specimen before the tests commenced.

The detailed heating and deformation procedure was carried out as follows:

(1) Each specimen was heated from ambient temperature to 1423 K at a steady rate of 10 K/s and held at this temperature for 3 minutes to achieve a uniform microstructure across the entire specimen.

(2) The temperature was then cooled to the preset deformation temperature at 10 K/s and maintained for 30 seconds to stabilize the temperature field.

(3) Compressive deformation was imposed at the predetermined strain rate until a maximum true strain of 0.7 was achieved.

(4) Immediately after the completion of deformation, the specimen was subjected to rapid water quenching to preserve the deformed microstructure for subsequent analysis.

The raw experimental data, including load-displacement and temperature-time curves, were collected in real-time by the testing machine. These data were then processed using specialized software to generate true stress-true strain curves for 316LN stainless steel under each of the tested deformation conditions.

3. Experimental Data Analysis and Constitutive Model Development

3.1 High-Temperature Flow Behavior

The true stress-true strain characteristics of 316LN stainless steel are strongly dependent on both deformation temperature and strain rate, as illustrated in Figure 1. At a constant true strain, the flow stress decreases significantly as the deformation temperature increases from 1273 K to 1423 K. This trend can be attributed to the enhanced thermal softening effects, primarily driven by dynamic recovery and dynamic recrystallization processes, which effectively counteract the work hardening induced by dislocation multiplication during deformation. Conversely, at a fixed temperature and true strain, the flow stress increases notably with higher strain rates. This behavior stems from the fact that the rate of dislocation generation during rapid deformation exceeds the rate at which dynamic softening mechanisms can mitigate their effects, leading to intensified work hardening.

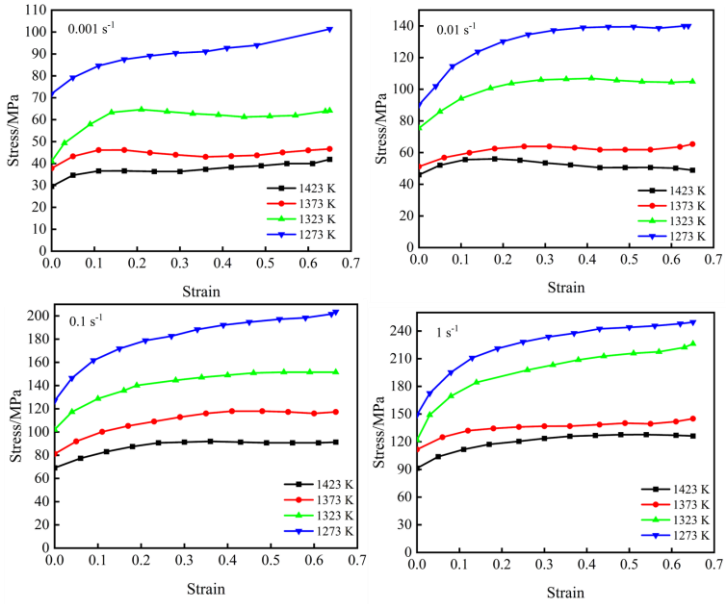

Figure 1. The true stress-true strain curves of 316LN stainless steel at different strain rates

Deeper investigation into the dynamic softening mechanisms indicates that 316LN austenitic stainless steel is subject to the coexistence of dynamic recovery and dynamic recrystallization during hot deformation. Dynamic recovery prevails at lower temperatures (e.g., 1273 K) or higher strain rates, leading to stress-strain curves

https://doi.org/10.64486/m.65.4.11

that exhibit a gently sloping profile following the initial rapid ascent. At higher temperatures (e.g., 1423 K) or lower strain rates, dynamic recrystallization is markedly intensified yet fails to fully counteract the work hardening effect, resulting in a continuous gradual increase in stress. These observations highlight the necessity of optimizing the temperature-strain rate combination to precisely regulate the microstructure and mechanical properties of 316LN stainless steel throughout the hot working processes [19–20].

3.2 Constitutive Model Establishment

The correlation among peak flow stress, strain rate, and temperature for 316LN stainless steel under high-temperature plastic deformation can be characterized by the Arrhenius model put forward by Sellars and Tegart, which integrates activation energy (Q) and temperature (T) as core parameters. This model is formulated through the following equations:

$$\dot{\varepsilon} = A_1\sigma^{n_1}\exp(\frac{-Q}{RT}) \text{ , (low stress level)} \tag{1}$$

$$\dot{\varepsilon} = A_2\exp(\beta\sigma)\exp(\frac{-Q}{RT}) \text{ , (high stress level)} \tag{2}$$

$$\dot{\varepsilon} = A\left[\sinh(\alpha\sigma)\right]^n\exp(\frac{-Q}{RT}) \text{ , (wide stress level)} \tag{3}$$

The Zener-Hollomon parameter (Z)-a strain rate parameter with temperature compensation-is incorporated to unify the impacts of temperature and strain rate:

$$Z = \dot{\varepsilon}\exp\left(\frac{Q}{RT}\right) = A\sinh(\alpha\sigma)^n \tag{4}$$

For a fixed temperature, combine Equations (1) and (2) to derive the constants n_1 and β by linear fitting of $\ln\dot{\varepsilon}$ vs. $\ln\sigma$ and $\ln\dot{\varepsilon}$ vs. σ plots (Figures 2 and 3), respectively. The constant α is then calculated as $\alpha = \beta/n_1$.

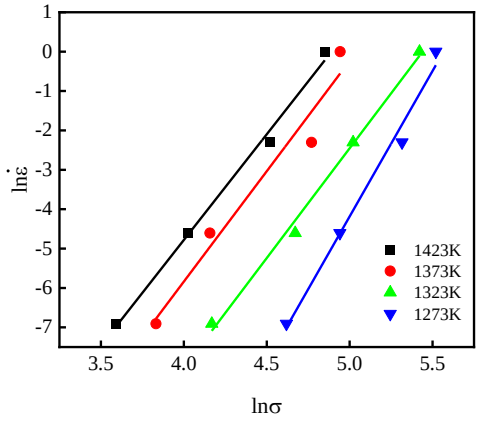

Figure 2. Relation curves of $\ln\dot{\varepsilon}$ and $\ln\sigma$

https://doi.org/10.64486/m.65.4.11

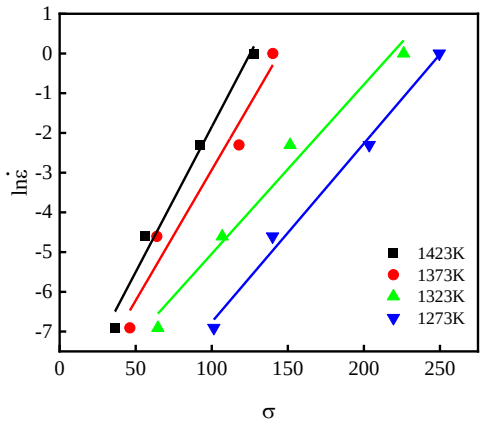

Figure 3. Relation curves of $\ln\dot{\varepsilon}$ and σ

For a fixed strain rate, use Equation (3) to calculate Q by linear fitting of $\ln\dot{\varepsilon}$ vs. $\mathrm{In}\left[\sinh(\alpha\sigma)\right]$ and $\mathrm{In}\left[\sinh(\alpha\sigma)\right]$ vs. 1000/T plots (Figures 4 and 5), respectively. The average values of the slopes obtained from the above fittings are n and K. $Q = nRK = 4.32 \times 0.008314\,\mathrm{kJ/mol} \times 19.189 \times 1000 = 689\,\mathrm{kJ/mol}$

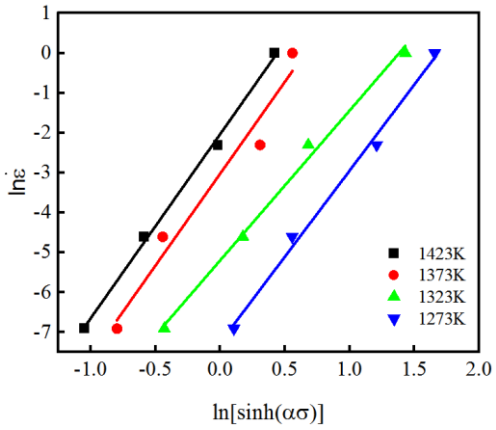

Figure 4. Relation curves of $\ln\dot{\varepsilon}$ and $\mathrm{In}\left[\sinh(\alpha\sigma)\right]$

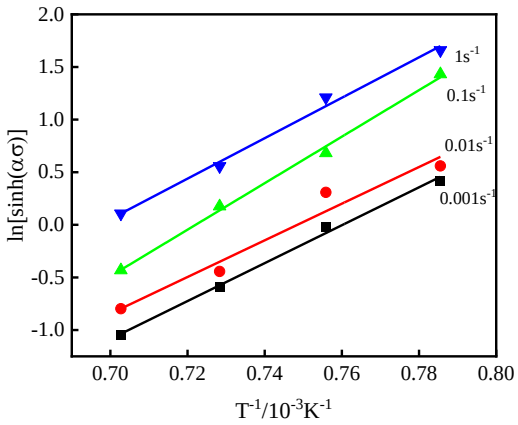

Figure 5. Relation curves of $\mathrm{In}\left[\sinh(\alpha\sigma)\right]$ and $1000/T$

Substitute the determined constants into Equation (4) and take the natural logarithm to obtain:

$$\ln Z = \ln A + n\sinh(\alpha\sigma) \tag{5}$$

Linear fitting of $\ln Z$ vs. $\mathrm{In}\left[\sinh(\alpha\sigma)\right]$ (Figure 6) provides the intercept $\ln A$, enabling the calculation of A.

https://doi.org/10.64486/m.65.4.11

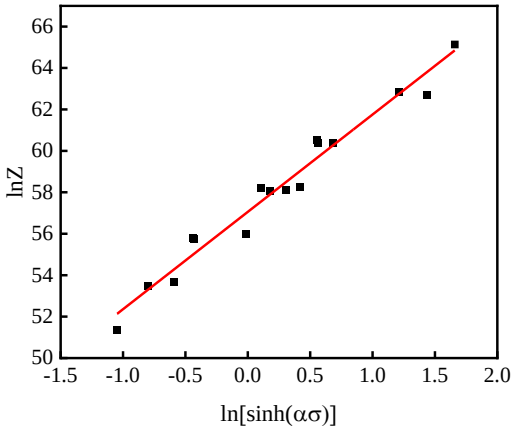

Figure 6. Relation curves of $\ln Z$ and $\ln\left[\sinh(\alpha\sigma)\right]$

3.3 Final Constitutive Model

Through the aforementioned linear regression analyses, the material constants for 316LN stainless steel were determined as follows: $\alpha = 0.00946\ \text{MPa}^{-1}$, $n = 4.32$, $Q = 689\text{kJ/mol}$, and $A=6.02\times10^{24}$. Thus, the constitutive model for 316LN stainless steel within the deformation temperature range of (1273–1423) K and strain rate range of (0.001–1) s^{-1} is:

$$\dot{\varepsilon} = 6.02\times10^{24}\left[\sinh(0.00946\sigma)\right]^{4.321}\exp(\frac{-689}{8.314T}) \tag{6}$$

where σ is in MPa and T is in K.

4. Model Validation and Simulation Analysis

4.1 Experimental Validation of the Constitutive Model

The development of the constitutive model for 316LN stainless steel is intended to forecast its deformation behavior under high-temperature rheological conditions. Hence, validating the applicability and precision of the established Arrhenius-type constitutive model for this material becomes essential. As illustrated in Figure 7, the correlation coefficient $R^2 = 0.97731$ between the predicted values and experimental data was derived through regression analysis of the flow stress results calculated by the proposed constitutive model. These findings demonstrate that the developed model can effectively characterize the flow behavior of 316LN stainless steel during high-temperature plastic deformation.

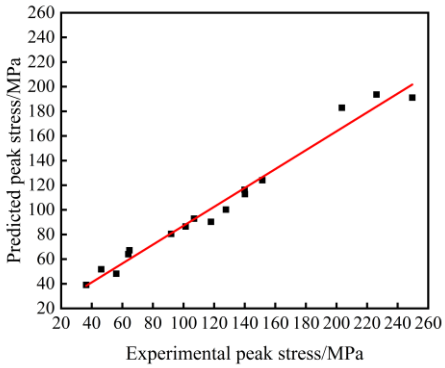

Figure 7. The calculation results of the predicted peak stress are compared with the measured values

https://doi.org/10.64486/m.65.4.11

4.2 Numerical Simulation Verification

The CATIA software was adopted to establish a model in accordance with the actual specimen dimensions of standard thermal simulation tests. The models of the upper punch, lower punch, and specimen were saved separately in STL format and then imported into the Deform-3D forming software. The specimen material was defined as a plastic material, using the newly established 316LN stainless steel; the upper and lower punches were defaulted to rigid materials; the specimen temperature and the movement speed of the upper punch were set to simulate the combinations of standard test data, respectively.

The deformation/heat conduction/recrystallization mode was selected, with a mesh division size ratio of 1, an ambient temperature of 20 °C, a convection coefficient of 0.02 N/(s·mm·°C) (≈ 20 W/(m²·K)), a mold temperature of 20 °C, and a shear friction type. The specimen was divided into tetrahedral elements using the mesh generation program built into Deform-3D. After the simulation was completed, the curve of the upper punch stroke versus load was exported. The transverse strain of the specimen was taken as the true strain. The radius of the contact surface between the specimen and the upper punch was then measured at a strain rate of $\dot{\varepsilon} = 0.05\ s^{-1}$. This radius was used as the instantaneous cross-sectional area for axial stress calculation to obtain the corresponding stress-strain data. A stress-strain curve derived from the simulation was constructed and juxtaposed with the experimental dataset, as illustrated in Figure 8.

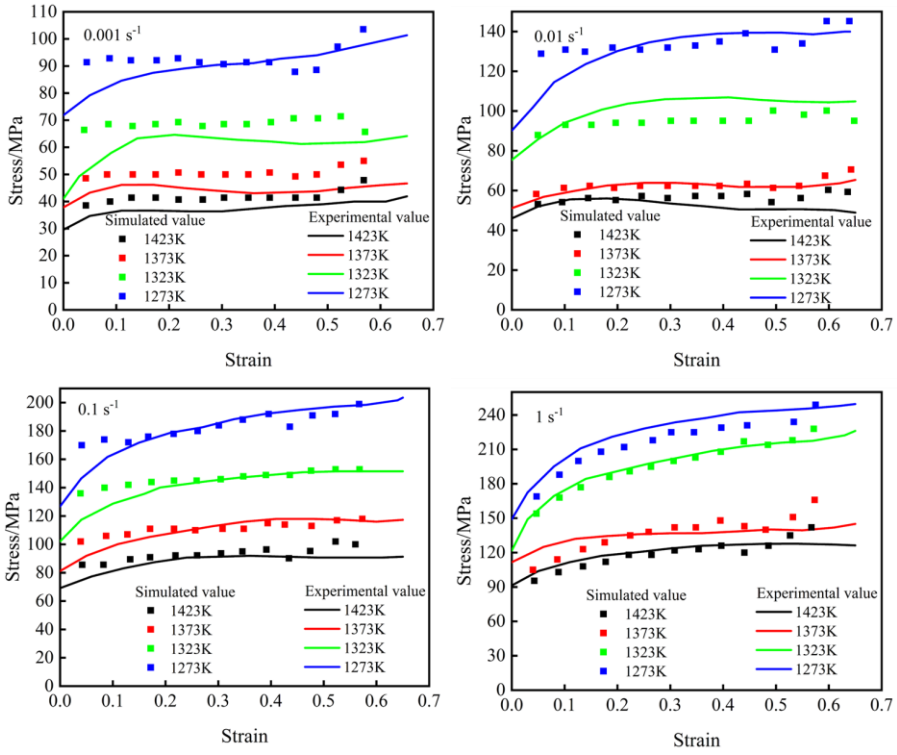

Figure 8. Simulated and experimental stress-strain curves of 316LN stainless steel during hot deformation

It is evident from Figure 8 that the simulated values exhibit excellent consistency with the experimental results, which verifies the reliability of the constructed simulation model and confirms its applicability to the research of engineering-associated die forging technologies.

https://doi.org/10.64486/m.65.4.11

5. Conclusions

Under the same strain rate, 316LN austenitic stainless steel exhibits a downward trend in compressive stress as deformation temperature rises; while at a fixed deformation temperature, its compressive stress increases alongside a higher strain rate. Analysis of the true stress-strain curves demonstrates that as strain accumulates, the material's compressive stress gradually stabilizes in the later stage of deformation. Leveraging the Arrhenius equation and natural logarithm linear regression method, this study determined the key material parameters of 316LN austenitic stainless steel during hot deformation, successfully developed a flow stress constitutive model, and validated its reliability. Additionally, combined with simulation analysis of standard hot simulation tests, the accuracy of the established material data and the feasibility of the simulation approach were further confirmed. The research outcomes offer theoretical insights and technical backing for optimizing the forming and processing technology of lightning rods used in ancient buildings.

Acknowledgments: Fund: the key project of the 14 th Five-Year Plan for Philosophy and Social Science Research in Shaoxing in 2025. Fund number: 145565.

References

[1] Li, Jingxiao, et al. "Investigation of lightning damage mechanism and flashover channels on glazed roofing tiles of ancient buildings through laboratory experiments." *Journal of Electrostatics*, vol. 110, pp. 103553, 2021, https://doi.org/10.1016/j.elstat.2021.103553.

[2] Li, Jingxiao, et al. "Study on the microscopic damage characteristics for glazed tiles of ancient buildings after lightning strike." *Journal of Cultural Heritage*, vol. 61, pp. 109-115, 2023, https://doi.org/10.1016/j.culher.2023.03.010.

[3] Li, Jingxiao, et al. "An experimental study of the damage degrees to ancient building timber caused by lightning strikes." *Journal of Electrostatics*, vol. 90, pp. 23-30, 2017, https://doi.org/10.1016/j.elstat.2017.08.009.

[4] Abbas, Adel T., et al. "An adaptive design for cost, quality and productivity-oriented sustainable machining of stainless steel 316." *Journal of materials research and technology*, vol. 9, no. 6, pp. 14568-14581, 2020, https://doi.org/10.1016/j.jmrt.2020.10.056.

[5] Rossi, Barbara. "Discussion on the use of stainless steel in constructions in view of sustainability." *Thin-Walled Structures*, vol. 83, pp. 182-189, 2014, https://doi.org/10.1016/j.tws.2014.01.021.

[6] Yan, Xiao-Li, et al. "Review of creep–fatigue endurance and life prediction of 316 stainless steels." *International Journal of Pressure Vessels and Piping*, vol. 126, pp. 17-28, 2015, https://doi.org/10.1016/j.ijpvp.2014.12.002.

[7] Song, Shin-Hyung. "A comparison study of constitutive equation, neural networks, and support vector regression for modeling hot deformation of 316L stainless steel." *Materials*, vol. 13, no. 17, pp. 3766, 2020, https://doi.org/10.3390/ma13173766.

[8] Gao, Fei, et al. "Flow behaviour and constitutive modeling for hot deformation of austenitic stainless steel." *Materials Research Express*, vol. 7, no. 11, pp. 116512, 2020, https://doi.org/10.1088/2053-1591/abb151.

[9] Liu, X. G., et al. "Study on hot deformation behaviour of 316LN austenitic stainless steel based on hot processing map." *Materials Science and Technology*, vol. 29, no. 1, pp. 24-29, 2013, https://doi.org/10.1179/1743284712y.0000000083.

[10] Chen, Le-li, et al. "Investigation on the hot deformation behavior of 316L stainless steel using 3D processing map." *Transactions of the Indian Institute of Metals*, vol. 72, no. 12, pp. 2997-3006, 2019, https://doi.org/10.1007/s12666-019-01674-4.

[11] Guo, Baofeng, et al. "Research on flow stress during hot deformation process and processing map for 316LN austenitic stainless steel." *Journal of Materials Engineering and Performance*, vol. 21, no. 7, pp. 1455-1461, 2012, https://doi.org/10.1007/s11665-011-0031-0.

 https://doi.org/10.64486/m.65.4.11

[12] Liu, Xin-gang, et al. "Prediction of critical conditions for dynamic recrystallization in 316LN austenitic steel." *Journal of Iron and Steel Research International*, vol. 23, no. 3, pp. 238-243, 2016, https://doi.org/10.1016/s1006-706x(16)30040-1.

[13] Wang, Shenglong, et al. "Study on the dynamic recrystallization model and mechanism of nuclear grade 316LN austenitic stainless steel." *Materials characterization*, vol. 118, pp. 92-101, 2016, https://doi.org/10.1016/j.matchar.2016.05.015.

[14] Xie, Gan Lin, et al. "Arrhenius-type Constitutive Model for 316LN Stainless Steel during Hot Deformation." *Materials Science Forum*, vol. 817, pp. 406-409, 2015, https://doi.org/10.4028/www.scientific.net/MSF.817.406.

[15] Kumar, Santosh, et al. "Analysis of elevated temperature flow behavior of 316LN stainless steel under compressive loading." *Transactions of the Indian Institute of Metals*, vol. 70, no. 7, pp. 1857-1867, 2017, https://doi.org/10.1007/s12666-016-0990-9.

[16] Ying Han, et al. "Investigation on hot deformation behavior of 00$Cr_{23}Ni_4N$ duplex stainless steel under medium-high strain rates." *Materials Characterization*, vol. 62, no. 2, pp. 198-203, 2010, https://doi.org/10.1016/j.matchar.2010.11.013.

[17] Xiao, H, et al. "Flow stress correction for hot compression of titanium alloys considering temperature gradient induced heterogeneous deformation." *Journal of Materials Processing Technology*, vol. 288, pp. 116868, 2021, https://doi.org/10.1016/j.jmatprotec.2020.116868.

[18] Ebrahimi, R., and A. Najafizadeh. "A new method for evaluation of friction in bulk metal forming." *Journal of Materials Processing Technology*, vol. 152, no. 2, pp. 136-143, 2004, https://doi.org/10.1016/j.jmatprotec.2004.03.029.

[19] Lvyunhui Shi, et al."The Effects of Hot-Deformed Microstructures on the Grain Boundary Character Distribution Evolution During Static Annealing in a 316L Stainless Steel." *Metallurgical and Materials Transactions A*, vol. 56, no. 11, pp. 1-19, 2025, https://doi.org/10.1007/S11661-025-07945-8.

[20] Zhang, Meng-xing, et al. "Influence of hot deformation on dynamic recrystallization behavior of a novel austenitic stainless steel: MX Zhang et al." *Journal of Iron and Steel Research International*, vol. 32, no. 12, pp. 4335-4349, 2025, https://doi.org/10.1007/S42243-025-01476-7

 https://doi.org/10.64486/m.65.4.11